EXPERIMENTAL AND FINITE ELEMENT ANALYSIS OF BONDLINE FLAW CRITICALITY IN COMPOSITE SCARF JOINTS

J. Kosmann[a,b*], D. Holzhüter[a], A. J. Gunnion[b,c], C. Hühne[a]

[a]*Institute of Composite Structures and Adaptive Systems, German Aerospace Centre (DLR),Braunschweig, Germany*
[b]*Cooperative Research Centre for Advanced Composite Structures, Melbourne, Australia*
[c]*Advanced Composite Structures Australia, Melbourne, Australia*
**jens.kosmann@dlr.de*

Keywords: Scarf repair, bonded repair, damage tolerance, finite element analysis

Abstract

Conventional design methods for bonded repairs to composite structure assume that the repair is in pristine condition. However, for a repair to be certified on primary structure, the repair must be designed to address damage tolerance and fatigue strength requirements, in addition to static strength. Therefore, the criticality of bondline flaws in composite scarf joints is analysed within this paper using finite element analysis (FEA). Experimental data is presented for scarf joints with various initial flaw sizes. As a result of both the experimental and FEA studies, it can be concluded that the strength of a scarf joint is considerably and adversely affected by the presence of a flaw.

1 Introduction

The widespread adoption of composite materials for primary aircraft structure, including wings and fuselage, presents a challenge for aircraft repair. Bonded repairs are generally preferable to bolted repairs for composite structure, yet their use is usually limited to non-critical applications as there is currently no accepted method to assess bond quality. For the adoption of bonded repairs to progress for primary structure, in addition to addressing concerns over so-called "kissing bonds", other performance requirements of the structure, including fatigue and damage tolerance, must be satisfactorily addressed. To date, there has been limited study of repair damage tolerance in literature. In this paper, criticality of flaws within the bondline of a bonded composite scarf repair is investigated using FEA and through tension testing of wide scarf joints with various size flaws.

MSC.Patran (Patran) was used for pre- and post-processing and the nonlinear FEA was performed in MSC.Marc (Marc). The process of creating a flaw, running and post-processing the analysis was automated through the use of the Python programming language and Patran Command Language (PCL). Tension test results, in combination with optical strain field measurements using the ARAMIS system from GOM mbH, are compared to the analysis.

2 Background of Bonded Scarf Repairs

Bonded repairs offer several advantages over bolted repairs for composite structure. For minor damage or repair of thin skin structures, external patch repairs are generally adequate. Scarf or stepped repairs are used in composite structures when high strength recovery is needed or when there is a requirement for a flush surface to satisfy aerodynamic or stealth requirements. Scarf repairs are complex to design and require the removal of significant parent

structure, particularly for thick skins due to the small scarf angles required to achieve the necessary strength recovery.

Although the damage tolerance of composite laminates is thoroughly investigated experimentally and numerically, there are limited studies on the damage tolerance of repairs in literature. Impact damage tolerance has been investigated [1-3]. Consideration of residual strength with pre-defined bondline flaws, for example that may correspond to manufacturing flaws or detection limits, is limited [4]. The flaws considered in this study conform with the latter, which are more amenable to examination by FEA. The scarf joints considered in ref. [4] contain flaws that run the entire width of the joint. In this study, the flaws are of partial width, closer approximating a discrete flaw within a larger repair.

Within the repair there are several failure modes that can lead to failure, including adhesive (interfacial) failure, cohesive failure (within the adhesive) and adherend failure (matrix failure, fibre failure and delamination). A robust process with appropriate controls should ideally prevent adhesive failure, and, provided the repair is well designed, the design case should typically be cohesive failure under hot/wet (HW) conditions. In this analysis, bondline flaws are approximated by removing elements from the bondline equal to the area of the flaw size. When assessing failure, only cohesive failure is considered in this present study.

3 Finite Element Analysis

An initial 2D mesh of the joint was created using a parametric modelling tool [7], and subsequently extruded with 3D elements to model the specimen. The term "2.5D" in this instance describes the model geometry, where, except for the flaw, the geometry is constant in the extruded direction (compared to a "full 3D" specimen, such as a circular repair in a panel). The analyses were undertaken with the material properties displayed in Table 1 and Table 2. The composite laminate is a 30 plies stacking of IM7/977-3 uni-directional prepreg, layup as follows: $[45/0/0/-45/90]_{3S}$.

Name	Symbol [Unit]	Value [RT]
Longitudinal modulus	E_{11} [MPa]	164100
Transverse modulus	E_{22} [MPa]	9860
In-plane shear modulus	$G_{12} = G_{31}$ [MPa]	4950
Out of-plane shear modulus	G_{23} [MPa]	2944
Poisson ratio	ν_{12}, ν_{23}	0.33, 0.34

Table 1: Summary of IM7/977-3 material data

The selected adhesive material in this study is the film adhesive FM300-2K. The performance is comparable to the FM300 film adhesive but with a relative low cure temperature of 120°C and service temperatures from -55°C to 150°C [5]. The assumed thickness of the adhesive in the model is set to 0.1 mm. To model different environmental conditions the properties of the adhesive varied for room temperature (RT) and HW conditions. The material models for the elastic-plastic adhesive cases in RT and HW is based on the data presented in the table below, derived from ref. [5], and implemented in Marc using a von Mises yield criterion.

Name	Symbol [Unit]	RT	HW [104ºC]
Shear modulus	G [MPa]	466	154
Poisson ratio	ν	0.3	0.3
Yield and Ultimate shear stress	τ_y, τ_u [MPa]	46.6, 54.4	12.3, 26.6
Yield and Ultimate shear strain	γ_y, γ_u	0.1, 0.85	0.08, 1.19

Table 2: FM300-2 data adopted in the FEA

3.1 Model Description

The nominal specimen geometry for the 2.5D model is summarised as follows:

- Specimen length = 150 mm
- Width = 75 mm
- Thickness = 30 x 0.13 mm (ply thickness) = 3.9 mm
- Scarf angle = 3° (centrally in the specimen located)
- Element size laminate = 0.41-1.6 x 0.13 x 0.63-5mm (length x height x width)
- Element size adhesive = 0.41 x 0.05 x 0.63-5mm (length x height x width)

A top view of the modelled scarf joint is displayed in **Figure 1**. As it is symmetric along the X-Y-plane only half of the joint is modelled to reduce the model size and reduce the runtime of the simulation. It is noted that due to the presence of +-45° plies, the material is not truly symmetric around this plane, however the resulting error is negligible and away from the area of interest. The flaw length is indicated with a length of d. The width of the flaw was kept constant at one third of the specimen width, i.e. 25 mm.

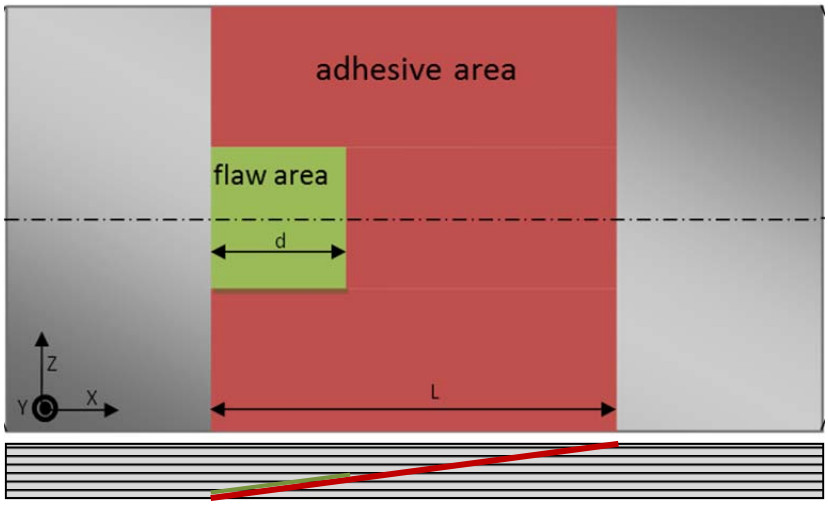

Figure 1: Top view on the 2.5D scarf Joint

3.2 Result Information

The strength of the joint was evaluated from the FEA by determining the load at which the bondline first reached the ultimate shear strain of the adhesive. An effective way of examining the adhesive strains is to consider the results of the nodes along the midplane of the adhesive [6]. The elastic-plastic failure criteria is ultimate strain, to allow the Marc solver to simulate also the steps after the initial failure, the material field allows the strain to exceed the ultimate strain of the original material. The final result is interpolated over the increment before and after the failure. For a qualitative illustration fringe plots are created. The fringe images showing the von Mises strain in the top view on the adhesive. The range is based on RT or HW conditions and fixed for all plots. The range is set to plot red colour over the maximum von Mises strain.

4 2.5D Joint Results (Partial-Width Flaw)

4.1 Effect on the Maximum load

The maximum strain anywhere in the middle of the bondline versus applied load for various flaw sizes is shown in **Figure 2** for RT (left) and HW (right).

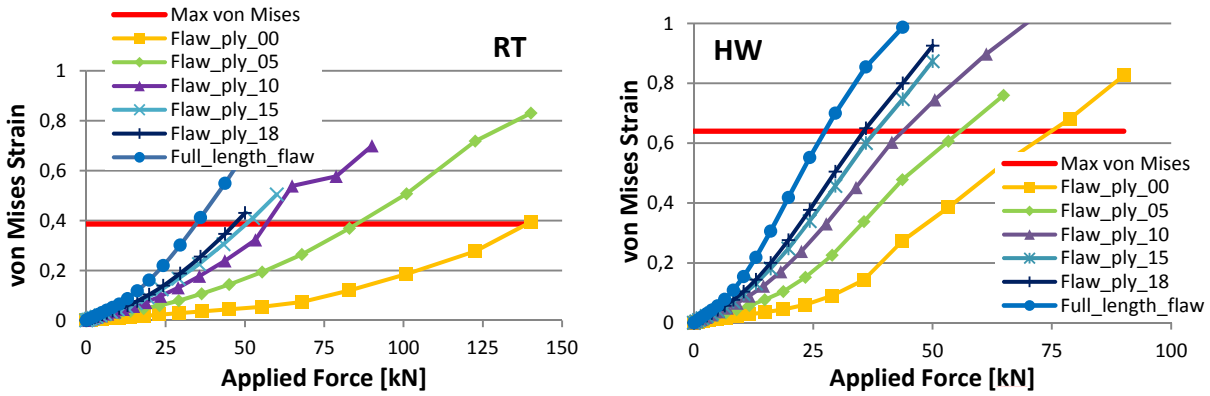

Figure 2: Effect of a bondline flaw on the maximum load for adhesive in RT and HW conditions

The effect of increasing flaw size on the joint strength is plotted in **Figure 3**. The results plotted in blue show a uniform stress model (i.e. where strength is directly proportional to effective bondline area), the results of the FEA for RT conditions shown in green and red for HW.

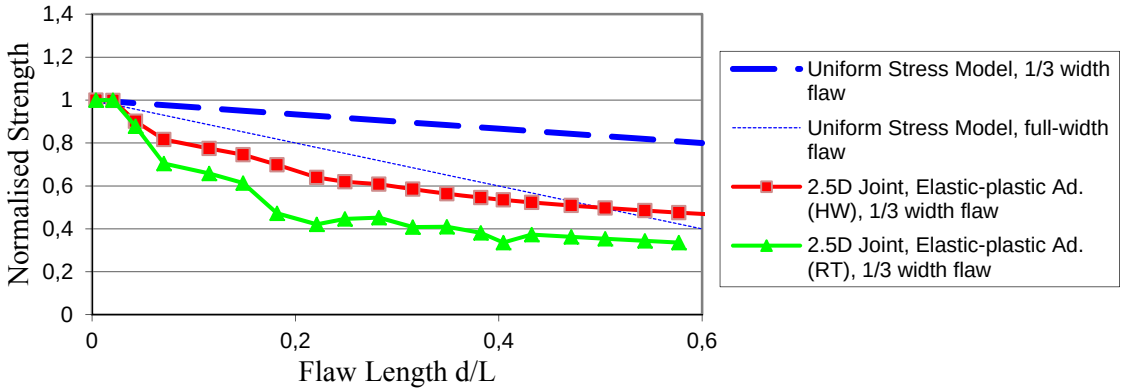

Figure 3: Normalised joint strength for various tip bondline flaw length ratios, 1/3 width

A fringe plot of the half bondline with various flaw sizes is given in **Figure 4** for HW conditions, taken at the load step after the ultimate von Mises strain was reached. The red circle on each fringe indicates the maximum strain position. For the case with zero flaw, there is a relative high strain value all across the adhesive, with peaks in the 0° plies and a minor influence of the symmetric boundary condition in the ±45° plies. For the flawed conditions, it can be seen that the highly stressed region of the bondline is more localised around the flaw, compared to the "No Flaw" case.

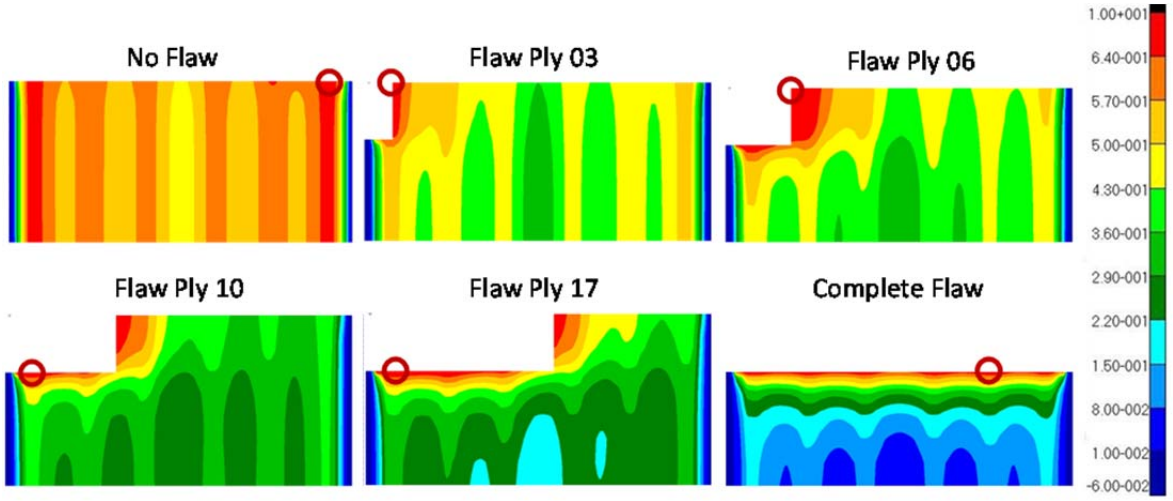

Figure 4: Fringe of the top view on the Adhesive in HW conditions

4.2 Discussion

From the FEA results the following conclusions can be made:

- The redistribution of load in the bondline shown in **Figure 4** reveals that the peak stresses generally occur to the side of the flaw, rather than at the ends of the flaw.
- Under HW conditions, the normalised strength versus the pristine condition is less adversely affected by the presence of a flaw compared to the RT case. However, as the HW strength will be much less than the RT strength, flawed HW condition is likely to still be critical.
- Using the adopted analysis methods and failure criterion, for the joint geometry considered, this result suggests that there is no benefit from load-by-pass effects.
- Plasticity in the bondline helps to reduce sensitivity to a flaw by redistributing localised stresses more broadly across the joint. The joint tolerance to flaws improves with increased plasticity (or toughness). However, the absolute strength of the joint may reduce as the yield stress of an adhesive typically reduces (say with temperature) as plasticity increases.

5 Experimental Validation of the 2.5D Analysis

5.1 Specimens manufacture

The 13 specimens for the flatwise tension testing in RT conditions were manufactured by the Cooperative Research Centre for Advanced Composite Structures (CRC-ACS), Melbourne. The composite layup and material are the same as in the FE model. The scarf region was machined using a CNC router. Practical limitations of the manufacturing process resulted in blunt tips, as show in **Figure 5(a),** revealing that the first 45° and two 0° are cut. The FE model was subsequently updated to reflect the blunt tips, assigning the elements in this region to the adhesive property set, as shown in **Figure 5(b)**. Flaws were introduced using Teflon film.

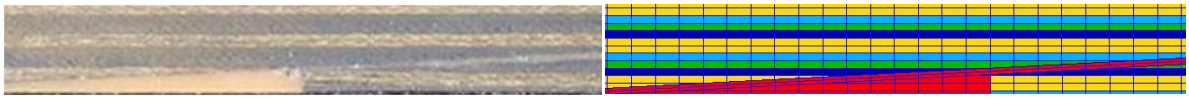

(a) (b)

Figure 5: (a) Image of scarf tip region of specimen, and (b) corresponding region of model after modification (red indicates adhesive material, blue 45°, yellow 0°plies and green 90°plies)

5.2 Tension Test Results

Initially, the focus should be on examining the ultimate load before the failure of the joint. **Figure 6** presents the average maximum load reached in the tension test and the corresponding deviation compared to the calculated failure load of the FE model. The average is built over specimens out of the same panel and with the same flaw size. It is obvious that the ultimate loads of the undamaged specimens are much smaller than predicted by FEM. Furthermore the difference between panel one and the panel two and three should be mentioned. With only around 82 kN compared to 131 kN panel one carries only 62% of Panel 2 and Panel 3. In the following analyses this effect is included in the result presentation and discussion.

Except for the largest flaw of 20x30mm all specimens have a lower ultimate load than predicted. The two specimens for the 20x30mm flaw are very close to the FEM analysis.

The pristine case and the 20mm wide flaws have been simulated with the modified FE model and the results added in **Figure 6**. The modified FEM analysis shows a clear strength reduction, especially for the pristine bondline. The strength of the modified tip is only 72% of the

original model. The effect on cases with a bondline flaw is less critical, especially for the 10mm long flaw.

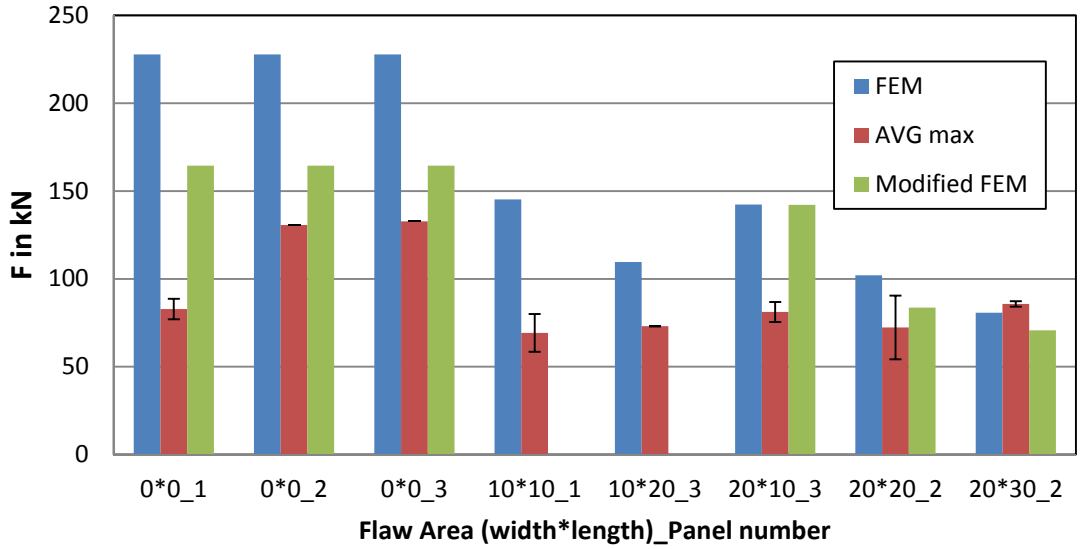

Figure 6: Maximum Load Tension Test vs. FEM and modified FEM

The analyses of the maximum failure load indicates that Panel 1 has the lowest strength. Inspection of the fracture surface shows no fiber or matrix failure in the specimen. In contract, the fracture surface of specimens from Panel 2 and 3 clearly shows fiber and matrix failure. This result suggests that the bond quality for Panel 1 is of a lower standard than Panels 2 and 3, although common materials and processes were applied for production of all specimens.

5.3 Front View ARAMIS Measurement

In the following images of the optical ARAMIS measurement the Epsilon X strain is analysed. The strain measurement shows clearly the end of the scarf and the overlapping adhesive, evident in the red line. In other scales also the scarf end on the back side and the areas were the 0° plies terminate in the scarf can be identified. In **Figure 7**, two stages of the specimen with 20x30 mm flaw are presented, the middle one is the last one before the failure occurs with a load of 83 kN and the left one is at 34 kN. On both images the upper line is the end of the overlapping adhesive or release film and has measurement errors but they are not important for the result. The end of the scarf is the second line. Compared to the undamaged specimens, the effect of the flaw in the bondline is very clear. In the left image a strain concentration next to the flaw can be identified. Furthermore the effect of the flaw on the adherend can be reflected by the strain on the outside of the laminate. A drop of the strain in the right image can be seen next to the side of the flaw which is interpreted as the beginning of the failure in the bondline. This location agrees with expectation from the FEA.

The graph of a cut through the scarf-end area shows the strain concentration next to the flaw and nearly no strain within the flaw area. Additionally the results of the modified FEA are plotted. The FE results are the X component of the strain in the nodes next to the scarf end. The upper load level is the on prior to failure, for both FEA and test, the second is around the half of the maximum FEA load.

This plot confirms the interpretation made of the images above and verifies the FEA results. For the step just before failure the strain distribution along the specimen width is higher for the test results but the maximum area is similar compared to the FE results. For a smaller load step the FE results are slightly above the test results but also here the results are very similar. The same effect can be analysed on specimens with smaller flaw sizes.

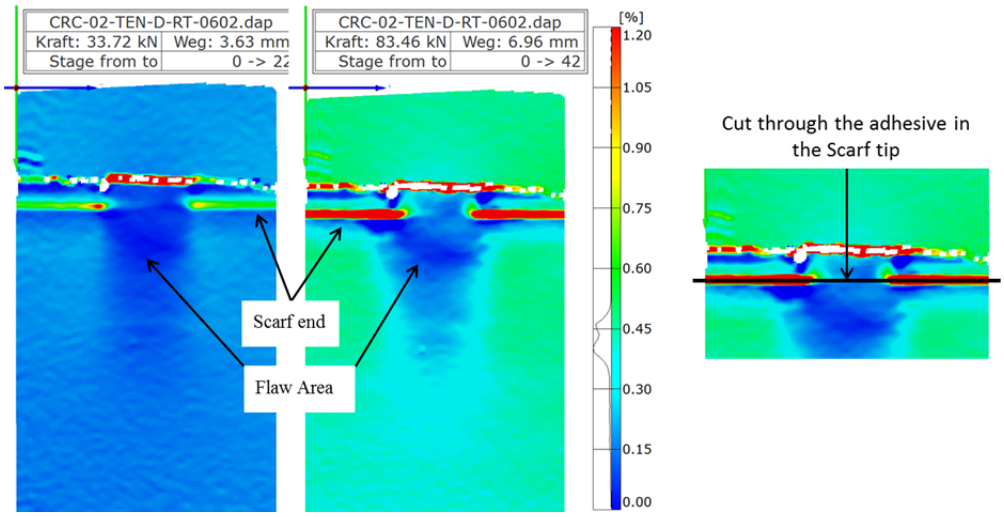

Figure 7: Specimen 0602 Epsilon X, left 34 kN middle 84 kN and right a cut through the scarf tip

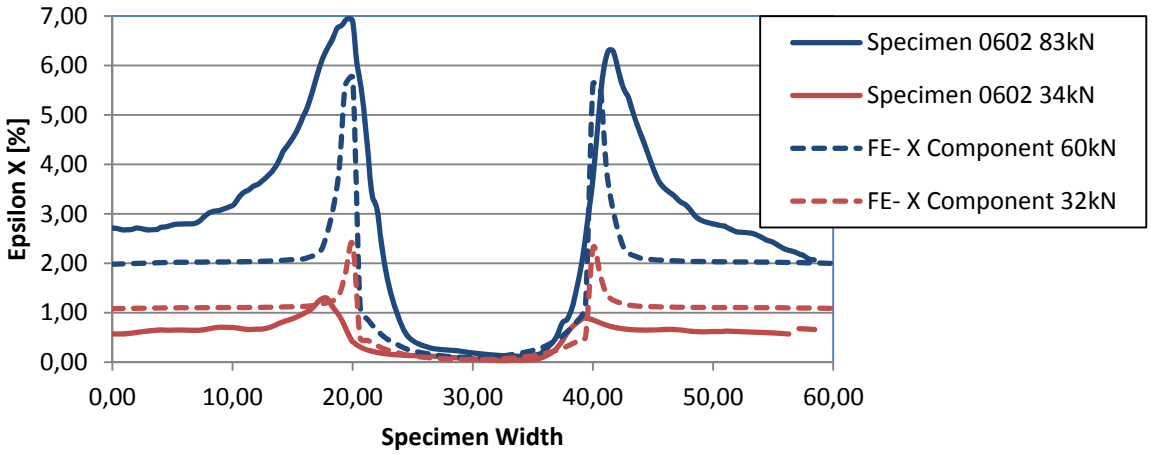

Figure 8: Cut through the Scarf end, Specimen 0602 Epsilon X and 20x30mm FE

5.4 Discussion

From the results presented for the tension test, the following conclusions can be made:

- The maximum load of the undamaged specimens is only 35 or 60% of the FEM calculations. If the blunt tip geometry is taken into account, with no other modifications, the results are changed toward the results of the test.
- The fracture images show different failure modes (eg. 90º ply failures at the interface), which will influence the difference in maximum load and is one reason for the differences to the FE results, which only consider cohesive failure.
- From the front view ARAMIS measurements showing the strain distribution over the scarf area, the flaw area can be readily detected. The strain results compare reasonably well with those expected from the FEA, as shown in **Figure 8**.

6 Conclusion and Recommendations

FEA studies showed that the presence of a bondline flaw considerably reduced the strength of a scarf joint, with the strength dropping greater than explained by the reduction in bond area alone. Comparisons between the RT and HW analysis results showed that under HW conditions, the normalised strength versus the pristine condition is less adversely affected by a flaw. However, as the HW strength will be much less than the RT strength (compare the yield strength values in Table 2), the flawed HW condition is likely to remain the critical case.

Tensile tests were successfully completed on RT specimens with various initial flaw sizes. Strain field measurements were made with the ARAMIS system, successfully capturing the influence of bondline flaws. The results showed that a bondline flaw causes a strain rise around the boundary of a flaw, and a reduction of strain over the flaw region.

Agreement between FEA and experiment was mixed. The general strain field behaviour observed in the ARAMIS data over the flaw agreed reasonably well with the FEA. The general trend in strength was captured, but the FEA initially over-predicted the experimental data, especially for the pristine condition. Introduction of blunt tips to better represent the as-manufactured specimens improved the agreement, but the strengths were still over-predicted. The strength predictions were based solely on cohesive failure, determined by the adhesive strain. Examination of the failure surfaces pointed to some mixed mode failures, with fibres breaking off around the interface. Improved analysis methods that consider adherend failure may be necessary to further improve accuracy of the strength predictions.

Further tension tests are planned for HW conditions. Once the test data becomes available, the modelling methods will be assessed against the failure loads witnessed in the tests. At elevated temperature, where the adhesive properties are considerably more affected than the laminate, it is likely that the failures will be dominated by cohesive failure. In which case, the FEA methodology described herein may show improved correlation with the experiment.

It should be appreciated that the strength reductions shown for the wide scarf joint specimens with flaws will not necessarily be reflected in real-life repairs, as the joints are a single load path structure, with limited ability load redistributed around a flaw. Further experimental and numerical work is recommended to assess implications for realistic repair scenarios.

Acknowledgements

This work was undertaken within the Robust Composite Repairs project, part of a CRC-ACS research program, established and supported under the Australian Government's Cooperative Research Centres Program. The authors would like to thank the CEO of DLR for facilitating this cooperation through financial support.

References

1. AB Harman, AN Rider, Impact damage tolerance of composite repairs to highly-loaded, high temperature composite structures, *Composites Part A: Applied Science and Manufacturing*, Volume 42, Issue 10, Pages 1321-1334, 2011.
2. AB Harman, CH. Wang. Damage tolerance and impact resistance of composite scarf joints, *Proceedings of the 16th International Conference on Composite Materials* (ICCM-16), Kyoto, 2007
3. I Herszberg, S Feih, AJ Gunnion and CH Henry, Impact damage tolerance of tension loaded bonded scarf repairs to CFRP laminates, *Proceedings of the 16th international conference on Composite Materials* (ICCM-16), Kyoto, 2007.
4. JY Goh, S Georgiadis, AC Orifici, CH Wang, Effects of bondline flaws on the damage tolerance of composite scarf joints, *Composites Part A: Applied Science and Manufacturing* 55, 110-119, 2013.
5. Cytec Engineering Material, FM300-2 Technical Datasheet, 2011.
6. AJ Gunnion, and I Herszberg, Parametric study of scarf joints in composite structures, *Composite Structures*, Volume 75, Issues 1-4, September 2006, Pages 364-376
7. J Wölper, D Holzhüter, C Hühne, Sizing Method for 3D modeled scarf joints using advanced finite element analysis, *Australasian Composites Conference*, Newcastle, April, 2014.